Root water gates and not changes in root structure provide new insights into plant physiological responses and adaptations to drought, flooding and salinity

Jean-Christophe Domec[a,b], John S. King[c], Mary J. Carmichael[d], Anna Treado Overby[e], Remi Wortemann R[f], William K. Smith[g] , Guofang Miao[h], Asko Noormets[i], Daniel M. Johnson[j]

Institution addresses:

[a]Bordeaux Sciences AGRO, UMR1391 ISPA INRA, 1 Cours du général de Gaulle 33175 Gradignan Cedex, France.

[b]Nicholas School of the Environment, Duke University, Durham, NC 27708, USA.

[c]Department of Forestry and Environmental Resources, North Carolina State University, Raleigh, NC 27606, USA.

[d]Departments of Biology and Environmental Studies, Hollins University, Roanoke, VA 24020, USA.

[e]Planning, Design and the Built Environment, Clemson University, Clemson, SC 29634, USA.

[f]Université de Lorraine, INRA, UMR 1434 Silva, 54000, Nancy, France.

[g]Department of Biology, Wake Forest University, Winston-Salem, NC 27109, USA.

[h]School of Geographical Sciences, Fujian Normal University, Fuzhou, FJ-350007, P.R. China.

[i]Department of Ecology and Conservation Biology, Texas A&M University, College Station, TX 77843, USA.

[j]Warnell School of Forestry and Natural Resources, University of Georgia, Athens, GA 30602, USA.

Corresponding author:

Jean-Christophe Domec / jc.domec@duke.edu

Running title:

aquaporins regulate plant response to environmental stresses

Word count:

Text body without M&M: 4361 words

7 figures, 6 in color.

2 Tables

Supplementary Data: 3 Figures

Highlight

New insights on organ hydraulics reveal that plant responses to drought, flooding and salinity is highly dynamic, reflecting a balance between species adaptive capacity and root aquaporin.

Abstract

The influence of aquaporin (AQP) activity on plant water movement remains unclear, especially in plants subject to unfavorable conditions. We applied a multitiered approach at a range of plant scales to (i) characterize the resistances controlling water transport under drought, flooding and flooding plus salinity conditions; (ii) quantify the respective effects of AQP activity and xylem structure on root (K_{root}), stem (K_{stem}) and leaf (K_{leaf}) conductances, and (iii) evaluate the impact of AQP-regulated transport capacity on gas exchange. We found that drought, flooding and flooding-salinity reduced K_{root} and root AQP activity in *Pinus taeda*, whereas K_{root} of the flood-tolerant *Taxodium distichum* did not decline under flooding. The extent of the AQP-control of transport efficiency varied among organs and species, ranging from 35%-55% in K_{root} to 10%-30% in K_{stem} and K_{leaf}. In response to treatments, AQP-mediated inhibition of K_{root} rather than changes in xylem acclimation controlled the fluctuations in K_{root}. The reduction in stomatal conductance and its sensitivity to vapor pressure deficit were direct responses to decreased whole-plant conductance triggered by lower K_{root} and larger resistance belowground. Our results provide new mechanistic and functional insights on plant hydraulics that are essential to quantifying the influences of future stress on ecosystem function.

Key words: aquaporin activity, anatomy, conductances, flooding, leaf water relations, plant hydraulics, water stress

Introduction

There is scientific consensus that the Earth's climate is changing at a geologically unprecedented rate and that human activities are a contributing factor, indicated by the National Academy of Sciences survey on climate change (NAS, 2020), and bolstered by a recent IPCC report (Oppenheimer et al., 2019). Due to a combination of seawater thermal expansion and melting of glaciers and polar ice sheets, global sea level rose 0.17 m over the 20th century and is projected to rise by at least 0.35 m by 2100 (Peltier, 2002). Coastal forests are among the world's most biologically diverse and productive ecosystems, but unfortunately are also the most vulnerable to sea level rise (SLR; Kirwan and Gedan, 2019). In addition to increased flooding, SLR is globally expected to foster high salinities into tributary freshwater areas of the coastal zones (Bhattachan et al., 2018). At the same time of being subject to increased salinity, those threatened ecosystems undergo periodic droughts exposing coastal forests to low soil water availability (DeSantis et al., 2007). Understanding forest responses to SLR therefore requires the determination of physiological response mechanisms to drought, flooding and flooding plus salinity.

Scientists have a broad-scale understanding of plant adjustment and tolerance to flooding and salinity along environmental gradients and the bulk of recent work in plants has been crucial in distinguishing adaptive plant strategies (Kirwan and Gedan, 2019). One of the most characteristic traits of wetland plants is aerenchyma, a specialized tissue made of intercellular gas-filled spaces that improves the storage and diffusion or oxygen. Overall, the physiological responses of plants to salt stress and flooding are similar in many ways (Allen et al., 1996; Munns, 2002), but the mechanisms by which plants deal with these stressors differ across species (Munns and Tester, 2008). The main consensus is that the primary responses of plants to flooding and salt is inhibition of root hydraulic conductance (Loustau et al., 1995; Rodríguez-Gamir et al., 2012).

In turn, this reduction in water uptake capacity reduces photosynthesis and growth due to the closure of stomata (McLeod et al., 1996; Munns and Tester, 2008). However, there are no studies that have focused on variation in hydraulic traits in contrasting species in terms of adaptive strategies and root physiological responses to full inundation, limiting our understanding of how they are linked to leaf- and whole-plant-level water transport, which limits our ability to predict forest ecophysiological response to SLR and climate change.

Water flow in the soil-plant-atmosphere continuum (SPAC) is determined by the hydraulic conductance of soil and plant tissues, which characterizes the structural capacity of the whole plant to move water (Tyree and Zimmermann, 2002). Hydraulic conductance (K_{plant}) is an important factor predicting gas exchange, transpiration, plant water status, growth rate and resistance to environmental stresses (Sperry, 2003; Addington et al., 2004; Brodribb and Holbrook, 2003; McCulloh et al., 2019). The partitioning of K_{plant} along the water transport path is very variable, not only among species, but also diurnally and among plant organs (Ye and Steudle, 2006; Johnson et al., 2016). Approximately 50-60% of the whole-plant hydraulic resistances ($1/K_{plant}$) are located in the root system, which shows the outstanding importance of this organ within the flow path (see review by Tyree and Zimmermann 2002). Peripheral organs such as leaves and roots have been proposed as possible replaceable hydraulic fuses of the SPAC during stress, uncoupling stems hydraulically from transpiring surfaces and soil (Hacke et al., 2000; Sperry, 2003; Domec et al., 2009 Johnson et al., 2016). Quantifying the relative contribution of K_{root} to K_{plant} and how it varies under drought, flooding, and flooding plus salinity is thus essential for understanding how these stressors influence photosynthesis and stomatal conductance (g_s) and their sensitivity to climatic variables. In addition, mechanistic depiction of variation in K_{plant} and its impact on g_s, and the

112 sensitivity of g_s to prominent environmental drivers, requires isolating the main resistances to plant
113 water flow, and their dynamics in response to abiotic stress factors, which has rarely been done.
114 Most research on abiotic stresses has focused on aboveground organs and neglected
115 physiological responses of the roots, especially in woody plants. This is surprising because
116 important processes of plant tolerance are located in the roots and also because roots are the first
117 organs to be affected by water stress, flooding and salinity (Krauss et al., 1999). In radial and axial
118 roots axes, resistance to water flow depends on root anatomy (Knifer and Fricke, 2011), whereas
119 in the radial component it is also a function of protein water channels, or aquaporins (AQP), that
120 regulate the resistance of the transcellular pathway (Chaumont et al., 2005; Gambetta et al., 2017).
121 Aquaporins are imbedded in the plasma and vacuolar membranes of most root cell types and form
122 pores that are highly selective for water (Tornroth-Horsefield et al., 2006). In crop plants AQP
123 chemical inhibitors (i.e. mercuric chloride or hydroxyl radicals) demonstrated that AQP down-
124 regulation is the principal cause of alterations of the radial pathway, resulting in a decrease in K_{root}
125 (Ehlert et al., 2009; Knifer and Fricke, 2011; Maurel and Nacry 2020). Despite a recent flurry of
126 studies, compared to reference plants used in molecular studies such as corn, tobacco and
127 *Arabidopsis* (Siefritz et al., 2002; Lopez et al., 2003; Bramley et al., 2009; Sade et al., 2010; Tan
128 and Zwiazek, 2019), the importance of species differences in AQP regulation in woody plants and
129 its effect within the SPAC is still poorly understood (McElrone et al., 2007; Gambetta et al., 2013;
130 Johnson et al., 2014; Rodriguez-Gamir et al., 2019).
131 Better information on physiological functioning of forest species in stressed environments
132 is needed to develop adaptive management strategies that will help protect threatened coastal
133 ecosystems (Carmichael and Smith, 2016). To fully understand the impacts of SLR on plant
134 adaptation, the influence of abiotic stresses on root hydraulics must be evaluated with respect to

the entire capacity of the plant to move water. This is especially relevant for seedlings, which have low physiological capacity to tolerate many stressors (Niinemets, 2010), impacting species persistence under changing conditions (Megonigal and Day, 1992; Brodersen et al., 2019). In that framework, our first objective was to characterize the vascular conductances that control water movement through the plant system under drought, flooding, and flooding plus salinity stresses. Our second objective was to quantify the effects of AQP activity on plant organs and partition the antagonistic effects of AQP and xylem structure on conductances. Our third objective was to evaluate a hypothesized correlation between leaf-level gas exchange and AQP regulation of water transport under varying environmental conditions. Using contrasting species, we tested the hypotheses that decrease in hydraulic conductance between treatments 1) is controlled by AQP activity rather than by a change in root xylem structure with greater declines in stress-intolerant plants, and in roots than in stems and leaves; and 2) is optimized in plants experiencing lower AQP inhibition, such that K_{root} exerts greater control on K_{plant}, which in turn affect g_s and carbon assimilation when environmentally stressed.

Material and Methods

Plant material and greenhouse experiments

We used 50 one-year-old *Taxodium distichum* L. and *Pinus taeda* L. half-sib seedlings supplied by ArborGen Inc. (Ridgeville, SC, USA). At the beginning of the spring season (late March), the seedlings were repotted in 19 liters commercial plant pots filled with a Fafard-4P soil mixture composed of sphagnum peat moss (50%), bark (25%), vermiculite (15%) and perlite (Fafard Inc., Agawam, MA, USA). This mixture was representative of the soil texture and organic matter content of soils found in coastal forested wetlands. Potted plants were maintained in a greenhouse

158 with a 16-h photoperiod where daytime mean temperature and relative humidity were kept at 23±3
159 ºC and 55±6 %, respectively. Before the treatments were applied, all 50 plants were watered three
160 times a week. Eight weeks after the beginning of the experiment 36 plants were randomly separated
161 into four groups (control, droughted, flooded, flooded plus salt) and were surrounded and buffered
162 by the 14 plants that were not used for the measurements. These treatments were intended to
163 represent stresses related to SLR and periodic droughts exposing coastal forests, and thus the soil
164 salinity treatment with no flooding was not studied. Those single-factor experiments were
165 conducted simultaneously and applied for 35 days (Rodriguez-Gamir et al., 2019). Control plants
166 were irrigated with 2 liters of water twice per week, which was enough to saturate the substrate.
167 For the drought treatment, plants were never irrigated from the start until the end of the experiment
168 (Rodriguez-Gamir et al., 2019). Flooding and flooding plus salinity was imposed by submerging
169 the seedlings to the root-collar (3 cm above the surface) without draining the pots (Pezeshki, 1992).
170 The salinity treatment (at a concentration of 4 g 1^{-1}, or 4 parts per thousand) was prepared using a
171 commercial seawater mixture (24 g 1^{-1} NaCl; 11 g 1^{-1} $MgCl_2$-$6H_2O$; 4 g 1^{-1} Na_2SO_4; 2 g 1^{-1} $CaCl_2$-
172 $6H_2O$; 0.7 g 1^{-1} KCl).
173
174 **Hydraulic conductance of root, shoot and whole plant**
175 Five weeks after the treatments were applied, root (K_{root}), shoot (K_{shoot}) and stem (K_{stem}) hydraulic
176 conductance were directly measured using a Hydraulic Conductance Flow Meter (HCFM; Tyree
177 et al., 1993) (Dynamax Inc., Houston, TX, USA). Hydraulic parameters were determined in six
178 loblolly pine and five bald cypress seedlings per treatment, and conductance values for a given
179 plant were obtained from the same plant. To minimize the potential impact of diurnal periodicity
180 on hydraulic conductance, all measurements were taken between 1000 hrs and 1200 hrs and under

the same environmental conditions (temperature of 22 °C, and relative humidity of 60%). During HCFM measurements, the leaves were submerged in water to maintain constant temperature and prevent transpiration. To measure K_{root} and K_{shoot} the plants were cut 5 cm above the soil surface and the cut ends of the shoots and roots were connected to the HCFM. This instrument perfuses degassed water through root or shoot system by applying pressure to a water-filled bladder contained within the unit. K_{root} was determined between 2 and 4 minutes after shoot decapitation, thus minimizing measurement errors to less than 10% (Vandeleur et al. 2014; Rodriguez-Gamir et al., 2019; see also Supplementary Figure 1). The flow rate of water through root or shoot was determined under transient mode (Yang and Tyree, 1994), which consists in measuring flow rate under increasing pressure applied by a nitrogen gas cylinder. Transients were also performed on shoots after removal of leaves to determine K_{stem}. The applied pressure gradually rose from 0 to 450 kPa over the course of approximately 1 minute and the flow rate at each pressure value was logged every 2 seconds using the Dynamax software. Hydraulic conductance (K) was then calculated using the formula: $K=Q_v/P$; where Q_v is the volumetric flow rate (kg s^{-1}) and P is the applied pressure (MPa). Hydraulic conductance was standardized to values for 25 °C to account for the effects of temperature on water viscosity. Because the HCFM operates under high pressure, the measured K_{root} and K_{shoot} represent maximum values of conductances, that is in the absence of embolized conduits. At the end of the measurements, all-sided leaf area of the shoots was determined with an LI-3100 leaf area meter (Li-Cor, Inc., Lincoln, NE, USA), and conductance values were expressed on leaf specific area basis (Yang and Tyree, 1994). All plant biomass fractions were then harvested and dried at 70ºC for 48 hours and weighed. Further, mass-specific root hydraulic conductance ($K_{root\text{-}biomass}$) was calculated by normalizing K_{root} by root dry mass.

Root (two opposite lateral roots per seedling taken about 2.5 cm down from the root collar were sampled) and stem tracheids were visualized by perfusing the decapitated samples with 0.1% toluidine blue and imaged at 90-180x magnification using a digital camera mounted on a widefield zoom stereo microscope (ZM-4TW3-FOR-9M AmScope, USA). Tracheid diameter was measured along four 4 radials rows per sample using an image analysis software (Motic Images version 3.2, Motic Corporation, China). In addition, the presence or absence of aerenchyma was assessed on 4 lateral roots per sample, which included the two used for tracheid size determination (no aerenchyma was present in the stems).

Whole plant hydraulic resistance was calculated as in Domec *et al.* (2016)

$$1/K_{plant}=1/K_{root}+1/K_{shoot} \quad (1)$$

and resistances of the shoot components ($1/K_{stem}$ and $1/K_{leaf}$) were calculated from the difference between resistances before and after removal of each leaf. Hydraulic conductance and resistance are reciprocals, and the latter is used for partitioning the resistances in the root-to-leaf continuum, and the former for examining the coordination between plant hydraulics and gas exchange.

Aquaporin contribution to hydraulic conductances

We quantified the AQP contribution to K_{root} and K_{shoot} (and its components) and K_{plant} using hydroxyl radicals (*OH) produced using the Fenton reaction (solution made by equal mixing of 0.6 mM H_2O_2 and 3mM $FeSO_4$) to inhibit AQP activity (Ye and Steudle, 2006; McElrone et al., 2007). Hydroxyl radicals has been shown to be less toxic and above all more effective in blocking water channels than mercuric chloride (Henzler and Steudle, 2004). Conductances with AQP function inhibited were measured by introducing approximately 18 ml of *OH solution, instead of water, into the existing compression couplings connected to the sample and the HCFM (McElrone

et al. 2007; Johnson et al. 2014). As previously measured (Almeida-Rodriguez, Hacke and Laur 2011; Rodriguez-Gamir et al., 2019), the effect of *OH on conductivity was effective and reversable in less than 6 minutes when radicals were replaced with distilled water (Supplementary Fig. 1). Six transient curves per sample were constructed with the HCFM: two before inhibiting AQP activity, two after AQP inhibition, and two final ones after flushing the samples with water only to reassessed flow rate with no AQP inhibition. We calculated the AQP contribution to K_{root}, K_{shoot} (K_{stem} and K_{leaf}) and K_{plant} as the difference between initial conductance and conductance after AQP inhibition, divided by the initial conductance (Rodriguez-Gamir et al., 2019).

From measurements of conductances before and after inhibiting AQP activity, we were able to calculate whether the departure in values from control was due to either the xylem-only (structural changes in xylem conduits) or the AQP-only part of the hydraulic pathway. For a given stress applied, the structural part of the hydraulic pathway reducing conductance was calculated by dividing the difference in conductance between control and treatment after inhibiting AQP activity by the difference in conductance between control and treatment without inhibiting AQP activity. The AQP effect was taken as 1 minus the structural effect.

Gas exchange and water potential

Net photosynthesis (A) and stomatal conductance (g_s) were measured with a Li-Cor 6400 (Li-Cor, Inc., Lincoln, NE, USA). For each leaf, the chamber was set to match prevailing environmental conditions assessed immediately prior to the measurement: atmospheric CO_2 concentration (390-410 ppm), relative humidity (46-59 %), photosynthetically active radiation (PAR; 1600-1800 µmol m^{-2} s^{-1}), and leaf temperature (21-26 °C). All gas exchange results were expressed on an all-sided leaf area basis, and only fully-expanded healthy-appearing needles of the same age were picked

for analysis. Maximum (light saturated) photosynthetic capacity (A_{sat}) was measured on 4 green branchlets needles per seedling grown in the upper third of the plants. Immediately after the gas exchange measurements were performed, leaf water potential (Ψ_{leaf}) was measured using a pressure chamber (PMS Ins., Albany, OR, USA). To assess maximum (least negative) Ψ_{leaf}, two branchlets per individual from each treatment were sampled at predawn (between 05:00 hrs and 06:00 hrs).

Net photosynthesis versus intercellular CO_2 concentrations (A-Ci curves) were measured at 25 °C leaf temperature, 60±10 % relative humidity and 1600 µmol m^{-2} s^{-1} PAR. The chamber CO_2 concentrations were set to ambient and sequentially lowered to 50 ppm and then to 1500 ppm. These data were used to estimate the maximum Rubisco carboxylation (V_{cmax25}), the maximum electron transport (J_{max25}), and the dark respiration (R_{d25}) rates according to Farquhar et al. (1980).

Field hydraulic and canopy conductance

Two contrasting sites were used to determine field values of K_{plant} and g_s under typical field conditions, droughted and flooded conditions of large trees growing in intact forests. Soil salinity never occurred at the field sites to our knowledge. The first study site is a forested wetland located at the Alligator River National Wildlife Refuge, on the Albemarle–Pamlico Peninsula of North Carolina, USA (35°47'N, 75°54'W). This research site was established in November 2008, and includes a 35-m instrumented tower for eddy covariance flux measurements, a micrometeorological station, and 13 vegetation plots spread over a 4km^2 area (Miao et al. 2013; Domec et al., 2015). The forest type is mixed hardwood swamp forest (>100-year-old); the overstory is predominantly composed of water tupelo (*Nyssa aquatica* L.) that represents 39% of the basal area and an even mix of red maple (*Acer rubrum* L.), bald cypress and loblolly pine. The

canopy of this site is fairly uniform with heights ranging from 16 m to 21 m, and with leaf area index peaking at 4.0 ± 0.3 in early July.

The second, drier site (35°11'N, 76°11'W) located within the lower coastal plain, mixed forest province of North Carolina (Domec et al., 2009). This 100-ha mid-rotation (23-year-old) loblolly pine stand (US-NC2 in the Ameriflux database) was established in 1992 and has an understory comprised of other woody species such as sparse red maple and bald cypress trees. Artificial drainage lowers the height of the water table, improving site access and increases productivity, especially during winter months (Domec et al., 2015).

At both sites, canopy conductance was derived from sapflow measurements and thus comprises the total water vapor transfer conductance from the 'average' stomata of the canopy. Sapflow was measured at breast height using thermal dissipation probes inserted in two flood-adapted species (bald cypress and water tupelo) and two others not adapted to flooding (red maple and loblolly pine) (see Domec et al., 2015 for further description of the sites and the methodology used). Note that water tupelo was only present at the wetland site. Stomatal conductance of the plants measured in the field was calculated from transpiration and vapor pressure deficit (VPD), using the simplification of the inversion of Penman–Monteith model (Ward et al., 2013). To analyze the effect of K_{plant} on g_s, K_{plant} from field and greenhouse samples was calculated from the slope of the relationship between diurnal variation in Ψ_{leaf} and transpiration (Loustau et al., 1995). Changes in Ψ_{leaf} from dawn to mid-afternoon were quantified with a pressure chamber (PMS, Albany, OR) on six to eight leaves collected from each tree equipped with sapflow sensors

Oren et al. (1999) showed that under saturated light, the decrease in g_s with increasing VPD is proportional to g_s at low VPD. Therefore, the sensitivity of the stomatal response to VPD when

PAR was above 800 µmol m^{-2} s^{-1} (light-saturated g_s) was determined by fitting the data to the functional form:

$$g_s = b - a \ln(VPD) \quad (2)$$

where b is g_s at VPD = 1 kPa (hereafter designated as reference or maximum canopy-averaged stomatal conductance, $g_{s\text{-}max}$), and a is the rate of stomatal closure and reflects the sensitivity of g_s to VPD [$dg_s/d\ln VPD$, in mmol m^{-2} s^{-1} $\ln(kPa)^{-1}$]. We propose to use this framework where VPD and light intensity are fixed to investigate the nature of the relationship between K_{plant} and $g_{s\text{-}max}$, and how this relationship affects the sensitivity of g_s to VPD.

Statistical analyses

All measured parameters were tested using multiple analysis of variance with species, treatments, and AQP activity taken as factors. Mean separation was performed using the Tukey's procedure at 95 % confidence level. Statistical analyses were run using SAS (Version 9.4, Cary, NC, USA) and curve fits using SigmaPlot (version 12.5, SPSS Inc. San Rafael, CA, USA).

Results

Plant biomass

All treatments significantly reduced loblolly pine (*Pinus taeda* L.) total biomass ($p<0.01$; Table 1), whereas for the flood-tolerant bald cypress (*Taxodium distichum* L.) only the drought and the flooded plus salinity treatments had a negative effect on growth ($p<0.037$). This decrease in plant growth was mainly attributed to a reduction in root and stem biomass in bald cypress ($p<0.032$), and in leaf and stem biomass in loblolly pine ($p<0.01$). Despite this reduction in plant size, the fine root to leaf mass ratio of bald cypress was only affected in the flooding plus salinity treatment,

316 whereas in loblolly pine it was stimulated by 25% and 55% in the flooding and the flooding plus
317 salinity conditions, respectively. All stresses decreased leaf mass per area (LMA) in loblolly pine
318 (p<0.02). In bald cypress LMA was only negatively affected by the drought and by the flooded
319 plus salinity treatments (p<0.01). Field measurements indicated that unlike loblolly pine and red
320 maple (*Acer rubrum* L.), flooded bald cypress and water tupelo (*Nyssa aquatica* L.) grew as rapidly
321 (p>0.65) as trees subjected to periodic or non-flooded conditions (Supplementary Fig. 2).
322
323 **Effect of flooding and salinity on the partitioning of hydraulic conductance**
324 All treatments decreased whole-plant hydraulic conductance (K_{plant}) in loblolly pine (p<0.05),
325 whereas bald cypress was only affected by the drought and the flooding plus salinity treatment
326 (Fig. 1). In both species the strongest decrease in root (K_{root}) and shoot (K_{shoot}) hydraulic
327 conductances were measured for plants subjected to flooding plus salinity. It should be noted that
328 flooding alone did not affect any of the conductances in bald cypress. When loblolly pines were
329 flooded, even K_{root} on a root-mass basis ($K_{root\_biomass}$) dropped significantly (by 45%), whereas K_{root}
330 or $K_{root\_biomass}$ of the flood-tolerant bald cypress did not (Table 2; Fig.1).
331 The overall decline in K_{plant} was mainly driven by an increase in root and stem resistances
332 in loblolly pine, and by root resistance only in bald cypress (Fig. 2). Under control conditions,
333 roots represented between 35% and 45% of whole-plant resistance ($1/K_{plant}$), and under treatments
334 this partitioning increased to more than 50% (p=0.038) in loblolly pine, which was paralleled by
335 a reduction in leaf resistance from 35% to 15% (p=0.023). In bald cypress, only the flooded plus
336 salt treatment increased the predominance of root resistance, which was accompanied by a
337 decrease in the contribution of leaf and stem to the overall whole-plant resistance.
338
339 **Aquaporin contribution to plant organ conductances and gas exchanges**

The reduction in K_{root} and K_{plant} between control and the other treatments (Fig. 2) was mainly caused by a reduction in AQP activity rather than by a change in root anatomy (Table 1; Fig. 3). Even when K_{root} was calculated on a root-biomass basis ($K_{root\text{-}biomass}$), the inhibition of AQP activity led to similar values of $K_{root\text{-}biomass}$ (AQP-inhibited $K_{root\_biomass}$ in Table 2) across all treatments (p>0.47) in bald cypress, and for the flooded treatment (p=0.87) in loblolly pine. Nonetheless, in loblolly pine seedlings, AQP-inhibited $K_{root\_biomass}$ decreased by 31% (p=0.042) and 45 % (p=0.028) in the drought and flooded plus salt treatments, respectively, but that was still less than the overall reduction in $K_{root\_biomass}$ (52 % and 66 %, respectively), indicating that changes in $K_{root\_biomass}$ were mostly driven by the inhibition of AQP. This reduction in $K_{root\_biomass}$ in loblolly pine mirrored the decrease in root and stem tracheid diameter in the drought and flooded plus salt treatments (Table 1). In bald cypress, tracheid size was not affected by treatment, but aerenchyma production was stimulated under flooded conditions (Table 1).

While blockage of AQP reduced hydraulic conductance, the extent of the decrease varied among organs and species (Fig. 3). Root AQP activity in loblolly pine decreased (p<0.001) from 42 % under controlled conditions, to less than 5-17 % in the different treatments, which was the driver of the decline in whole-plant AQP contribution (Fig. 4A). In this species, we found that flooding and flooding plus salinity reduced the AQP activity of the whole plants from 32 % to less than 6 % (p<0.01). In bald cypress only the drought and flooded plus salt treatments reduced (p<0.02) AQP contribution to K_{root} or K_{plant} (Fig. 4B). For that species, the inhibition of AQP in the flooding treatment did not affect (p=0.95) K_{root} or K_{leaf}. In both species, drought also had a significant effect on AQP contribution to K_{leaf} with a decrease from 17 % to 9 % (p<0.03) in loblolly pine, and from 44 % to 23 % (p<0.001) in bald cypress. In both species there was no treatment effect on the contribution of AQP activity to K_{stem} (p>0.42).

Maximum stomatal conductance ($g_{s\text{-}max}$; i.e. g_s measured at a reference VPD of 1kPa and under saturated light) for bald cypress was only negatively affected by drought and the flooding plus salt treatment (Table 2). In loblolly pines, $g_{s\text{-}max}$ differed under flooded and flooded plus salt treatments, experiencing the smallest and the largest stomatal closure, respectively. Photosynthetic rate of both species was also negatively affected by treatments (p<0.04), with the strongest reduction for the drought and flooded-salt treatments (Table 2). The disruption of photosynthesis concurred with a reduction in rubisco carboxylating enzyme activities and maximum electron transport rate (VC_{max25} and J_{max25}, respectively; Table 2). Similarly, across species dark respiration rates were only affected by the flooded plus salt treatments.

After taking into account the effect of VPD on g_s, K_{plant} had a major influence on $g_{s\text{-}max}$ at field conditions. Across species and treatments, and whether plants were from the greenhouse or grown in the field, a 50% reduction in K_{plant} was accompanied by a 37 % decline in $g_{s\text{-}max}$ (Fig. 5A). There was indeed no difference (p=0.33) in the relationship between $g_{s\text{-}max}$ and K_{plant} for seedlings growing in greenhouse and mature trees in the field. Species differences were apparent in K_{plant}, with higher values in bald cypress and red maple. Flooded loblolly pine exhibited the same level of reduced K_{plant} as water-stressed plants. In red maple, permanently flooded conditions reduced water uptake capacity more than two-fold, and this species exhibited higher hydraulic limitation and $g_{s\text{-}max}$ in flooded than in drought-stressed conditions. However, bald cypress and water tupelo (circles and diamonds in Fig. 5A, respectively), which are species found in permanently wet soils, did not experience more than 15 % decline in $g_{s\text{-}max}$ under flooded conditions. The sensitivity of g_s to VPD was linearly related to $g_{s\text{-}max}$ (Fig. 5B) and K_{plant} (Supplementary Fig. 3). Stomatal conductance declined in response to increasing VPD, and the magnitude of the reduction varied over the measurement period as shown by the decline in $g_{s\text{-}max}$.

386 The slope of the relationship between $g_{s\text{-}max}$ and the sensitivity of g_s to VPD (0.62 ± 0.04) was not
387 different (p>0.99) than the previously reported generic value of 0.60 based on a hydraulic model
388 that assumes tight stomatal regulation of Ψ_{leaf} (Oren et al., 1999).

389 Maximum g_s and stomatal sensitivity to VPD decreased linearly with increasing the
390 contribution of root hydraulic resistance ($1/K_{root}$) to $1/K_{plant}$ for both species (Fig. 6). Those
391 negative relationships appeared also to be identical across treatments with a 50 % increase in
392 resistance belowground resulting in a 56 % reduction in g_{s_max} and in a 65 % decrease in stomatal
393 sensitivity to VPD.

394 The decrease in g_{s_max} and A_{sat} were linked to a decrease in AQP contribution to root
395 conductance among treatments and also species (p<0.039; Fig. 7). Although weaker, those
396 relationships still held when whole-plant AQP activity was compared to gas exchange, and a 25
397 % decrease in AQP contribution to K_{plant} was predicted to reduce g_{s_max} by 38% and A_{sat} by 30 %.
398

399 ## Discussion

400 In US coastal regions from Maryland to Texas that are vulnerable to SLR (Titus and Richman,
401 2001; Kirwan and Gedan, 2019), many species such as bald cypress, water tupelo, red maple and
402 loblolly pine are ecologically dominant and commercially important. The first two species are fully
403 adapted to partial or total soil flooding and the other species are common to forest communities of
404 estuarine woodlands (Pezeshki, 1992; Keeland and Sharitz, 1995). Bald cypress seedlings
405 generally tolerate flooding, but marked with an initial reduction in growth (Allen et al., 1996).
406 However, within 3 to 5 years, seedlings generally recover from the stress imposed by developing
407 pneumatophores (Megonigal and Day, 1992), explaining why flooded trees may grow as rapidly
408 as trees subjected to non-flooded conditions (Supplementary Fig. 2). However, before this root

409 formation occurs, the influence of AQP on control of plant water movement and gas exchanges is
410 needed and reflected in our results (Fig 4; Fig.7).
411
412 **Aquaporin activity appears to be essential in species-specific tolerance to stress**
413 Our results highlight the integrated nature of hydraulics across the whole plant and emphasized
414 the contributions of structural and physiological components to conductance (Bramley et al., 2009;
415 Maurel and Nacry, 2020). Drought, flooding and flooding plus salinity treatments caused a
416 significant shift in hydraulic resistance away from stem and leaves to the roots, because of
417 differential transmembrane AQP activity and not because of changes in the apoplastic hydraulic
418 pathway (xylem diameter) (Table 1, Fig. 3 and see AQP-inhibited $K_{root\_biomass}$ in Table 2). During
419 stress, some structural and anatomical changes also occurred as seen by the decrease in either leaf,
420 stem or root biomass under drought or flooded plus salt treatments, affecting for the latter treatment
421 root to leaf area ratio in both species (Table 1). However and unlike the role played by AQP, those
422 structural changes provided only minute adjustments in xylem hydraulic conductance
423 (conductance once AQP activity was inhibited) and did not explain the whole decrease in
424 conductance and thus the physiological mechanisms controlling water transport through the root
425 (Table 2; Fig. 3). Both loblolly pine and bald cypress were highly susceptible to the combined
426 stress of flooding plus salinity which lends support to the role of saltwater intrusion in the
427 formation of coastal ghost forests, since bald cypress is also dying in these forests (Kirwan and
428 Gedan, 2019). Lower predawn Ψ_{leaf} were expected with higher salinity because the lower osmotic
429 potential of the medium (4 ppm corresponding to an osmotic potential of 0.31 MPa) likely
430 increased leaf tissue ionic concentration (Allen et al., 1996). This excess of ions disrupted
431 photosynthesis and inhibited carboxylating enzyme activities (Table 2), which in turn contributed

to inhibited root or leaf growth, and the production of new aerenchymatous roots in the flood-adapted species (Table 1).

These findings may shed light on the adaptive advantages of altering AQP activity in response to environmental stresses (Maurel and Nacry, 2020). Regarding drought, lowering AQP activity in roots should lead to larger Ψ_{leaf} gradients, inducing stomata to close more rapidly. Reducing water channel activity can then be seen as a means to reduce water loss when soil water availability is low (McLean et al., 2011). In the case of flooding, the resulting decrease in K_{root} observed in the flood-intolerant species (such as loblolly pine used here) could also limit water transport to the leaves, causing stomatal closure and thus protecting the integrity of the whole hydraulic system until non-stressed conditions resume (Else et al., 2001). Loblolly pine is known to be tolerant to low salinity and short-term flooding (Poulter et al., 2008), and our experiment showed that this species reduced significantly gas exchange under these conditions, but to levels that were not lethal (Table 2). The negative impact of flooding on plants is a consequence of the low solubility of oxygen in water (Leyton and Rousseau, 1958), leading to anoxia (Kozlowski, 1997). The tight coupling of AQP functioning to the drop in cell energy (due to oxygen deprivation and acidosis) suggests that short-term adjustments in tissue hydraulics are critically needed during the early stages of the anoxic stress to balance water uptake with water loss (Tan et al., 2019). Long-term metabolic adaptation to flooding is generally characterized by the decrease in belowground biomass to limit oxygen deficiency, but one of the most adaptive features of plants of wetland ecosystems is aerenchymatous tissues characterized by intercellular gas-filled spaces that improve the storage and diffusion of oxygen. Unlike the adjustment in root biomass or xylem anatomy that can take more than 2 months (Krauss et al., 1999) and was not observed in any of the two seedlings (Table 1), intercellular air spaces, which were present after 5 weeks of flooding

in bald cypress, likely played a vital role in maintaining root uptake and preventing the AQP-mediated reduction in K_{root}. Kamaluddin and Zwiazek (2002) and Holbrook and Zwieniecki (2003) have also proposed that anoxia-induced AQP down-regulation may prevent the transport of ethylene precursors away from the root, thereby favoring the accumulation of ethylene to trigger the differentiation of root aerenchymas, especially in adapted species such as bald cypress (Table 1). Salinity added to the flooding stress may trigger larger AQP inhibition, so that advective salt flow to the root surface may be minimized (Azaizeh and Steudle, 1991). In the short term (a few hours following exposure to flooding or flooding plus salinity), it has been shown that plants respond to osmotic shock by reduced AQP activity (Martinez-Ballesta et al., 2000; Rodríguez-Gamir et al., 2012), which in our case was followed by reduced K_{root}, most likely as an adaptive strategy to eliminate water loss from the roots under conditions of low osmotic potential.

Finally, it can also be hypothesized that the role of AQP may in fact not concern the primary response of the plant to stress, but its recovery performance (Siefritz et al., 2002). Stimulation of specific AQP suggested that "gating" in response to salt stress involved not only the reduction in water channels, but also an enhancement in the internalization of specific AQPs (raft–associated pathway), putatively becoming active once stress is relieved (Li et al., 2011).

Root hydraulics as related to whole plant water transport and gas exchange

One of the objectives of our study was to evaluate a hypothesized correlation between leaf gas exchange and root hydraulics as influenced by AQP activity. The decline in g_{s_max} (and it is sensitivity to VPD) and photosynthesis was strongly related to the increase in root resistance due to a decrease in AQP contribution to K_{root}, with a common relationship found among the species despite important differences in treatment responses (Figs. 6 and 7). In non woody plants, it has

been suggested that abscisic acid (ABA) accumulation in leaves may be responsible for stomatal closure in flooded plants (Castonguay et al., 1993; Else et al., 2001). However, in woody plants the marked reduction in g_s in flooded seedlings does not seem to be induced by ABA, since a significant reduction in g_s appeared a week after stressors were applied (unpublished data; Rodríguez-Gamir et al., 2012), whereas the increase in ABA in leaves is generally detected 4-5 weeks later (Zhang and Zhang, 1994; Rodríguez-Gamir et al., 2012). Maximum g_s and K_{plant} were tightly coordinated in plants growing in the field or in greenhouse (Fig. 5). Changes in K_{plant}, driven by K_{root}, imposed a decline in g_{s_max}, thus affecting leaf water status and further increases in transpirational water loss and carbon assimilation. Midday Ψ_{leaf} did not change during the flooding treatment, highlighting the adaptive role of stomatal closure in counteracting leaf dehydration (Meinzer, 2003). Furthermore, our data indicate that flooded pines exhibited the same level of reduced K_{plant} as water stressed plants. Field data showed that red maple exhibited higher hydraulic limitation and higher $g_{s\text{-}max}$ in flooded than in water stressed conditions, indicating that species differences exist in the response to flooding. In contrast, bald cypress and water tupelo regulated very efficiently the closure of stomata, thus adjusting the evaporative water losses to the water uptake capacity of roots and the resulting decrease in K_{plant} (Fig. 5).

Our results also showed that the sensitivity of g_s to VPD was mostly attributable to the variation in $g_{s\text{-}max}$, which is consistent with the isohydric regulation of Ψ_{leaf} induced by K_{plant} (Oren et al., 1999). Stomata responded to VPD in a manner consistent with protecting xylem integrity and thus the capacity for water transport (Domec et al., 2009; McCulloh et al., 2019). Future climate change is expected to increase temperature and therefore VPD in many regions (Oppenheimer et al., 2019). Stomatal acclimation to VPD as affected by drought, flooding and flooding plus salinity could potentially have a large impact on the global water and carbon cycles.

Here we measured that in forested wetlands global plant transpiration responses to future climate will probably not differ from expectations based on the well-known relationship between g_s and VPD (Oren et al., 1999). To improve climate predictions of warming effects on transpiration for plants subjected to different abiotic stresses, our results indicated that modelers could potentially allow for predictable shifts in g_s under water stress but also flooded conditions, combined with the use of single coefficient conveying g_s sensitivity to VPD.

Woody species responses to flooding and flooding plus salinity are wide-ranging and can change based on the life-history stage of a plant. Seedlings are generally more sensitive to salinity while mature plants may show a wider range of tolerance (Kozlowski, 1997). However, when our field and greenhouse observations were analyzed together, some common responses were observed (Fig. 5), highlighting the need for integrating data on seedlings and mature plants in future studies on wetland adaptation to SLR and its restoration (Carmichael and Smith, 2016).

Conclusion

Our study provides new functional and mechanistic insights on plant hydraulics by showing that the components of K_{plant} are highly dynamic, reflecting a balance between species adaptive capacity and AQP functioning. Neither species tolerated flooding plus salinity. In loblolly pine, high water uptake was largely mediated by active transport through AQP, but was easily disrupted by drought, flooding and salinity. In bald cypress, a flooded-tolerant species, AQP contribution to water transport was less sensitive overall and did not respond to flooding. Under controlled conditions, AQP activity and xylem structure were colimiting root water transport. However, in response to environmental factors, except again for the flooding treatment in bald cypress, AQP functioning rather than changes in xylem structure or biomass allocation controlled the fluctuations

524 in K_{root}, and thus in K_{plant}. The decline in K_{leaf} was rather the consequence of both a decrease in
525 AQP activity and in structural changes. An important challenge was also to integrate the AQP-
526 mediated reduction in K_{root} within the mutual interactions of roots and shoots and its putative effect
527 on gas exchange. As such, across species and treatments, the reduction in g_s and its sensitivity to
528 VPD appeared to be direct responses to decreased K_{plant} and was influenced by AQP contribution
529 to water transport.
530

531 **Data availability statement**
532
533 The data supporting the findings of this study are available from the corresponding author (Jean-
534 Christophe Domec) upon request.
535
536 **Funding information:** This work was supported by a grant USDA-AFRI (#2012-00857), the
537 National Science Foundation - Division of Integrative Organismal Systems (#1754893), and by
538 the ANR projects CWSSEA- SEA-Europe, and PRIMA-SWATCH. The USFWS Alligator River
539 National Wildlife Refuge provided the forested wetland research site, and in-kind support of field
540 operations.
541
542 **Author contributions:** J.-C.D. and D.M.J. conceived the original screening and research plans;
543 J.-C.D., D.M.J., R.W. and M.J.C. performed the hydraulics experiments, A.T.O., M.J.C. and R.W.
544 performed the gas exchange experiments; J.S.K., J.-C.D., A.N., and G.M. performed field
545 experiments; W.K.S. provided plant materials; J-C.D. and D.M.J. analyzed the data and wrote the
546 article with contributions of all the authors.
547

548 **References**
549 **Addington RN, RJ Mitchell, R Oren and LA. Donovan** (2004) Stomatal sensitivity to vapor
550 pressure deficit and its relationship to hydraulic conductance in *Pinus palustris.* Tree Physiology
551 **24**:561–569.
552
553 **Allen JA, Pezeshki S R, Chambers J L** (1996) Interactions of flooding and salinity stress on
554 baldcypress (*Taxodium distichum*). Tree Physiology **16**: 307-313.
555
556 **Almeida-Rodriguez A.M., Hacke U.G, Laur J.** (2011) Influence of evaporative demand on
557 aquaporin expression and root hydraulics of hybrid poplar. Plant, Cell Enviro 34:1318-1331
558
559 **Azaizeh H and E Steudle** (1991) Effects of salinity on water transport of excised maize (*Zea mays*
560 L.) roots. Plant Physiology **97**: 1136–1145.
561

Bhattachan A ., R. E. Emanuel, M. Ardón, E. Bernhardt, S.M. Anderson, M.G. Stillwagon E.A. Ury, T.K. BenDor, and J. P. Wright (2018). Evaluating the effects of land-use change and future climate change on vulnerability of coastal landscapes to salwater intrusion. Elementa Sciences of the Anthropocene **6**:62.

Bramley H, Turner NC, Turner DW, Tyerman SD. 2009. Roles of morphology, anatomy, and aquaporins in determining contrasting hydraulic behavior of roots. Plant Physiology **150**, 348–364.

Brodersen CR, Germino MJ, Johnson DM, Reinhardt K, Smith WK, Resler LM, Bader MY, Sala A, Kueppers LM, Broll G, Cairns DM, Holtmeier F-K and Wieser G (2019) Seedling Survival at Timberline Is Critical to Conifer Mountain Forest Elevation and Extent. Front. For. Glob. Change **2**:9. DOI: 10.3389/ffgc.2019.00009

Brodribb TJ and NM Holbrook (2003) Stomatal closure during leaf dehydration, correlation with other leaf physiological traits. Plant Physiology **132**, 2199-2173.

Carmichael MJ and Smith WK (2016) Growing season ecophysiology of *Taxodium distichum* (L.) Rich. (bald cypress) saplings in a restored wetland: a baseline for restoration practice. Botany **94**: 1115-1125.DOI: 10.1139/cjb-2016-0147.

Castonguay Y., Nadeau P, Simard R.R (1993) Effects of flooding on carbohydrate and ABA levels in roots and shoots of alfalfa, Plant Cell Environ **16**: 695-702.

Chaumont F, Moshelion M, Daniels MJ. 2005. Regulation of plant aquaporin activity. Biology of the Cell **97**: 749–764

Church JA, P Huybrechts, M Kuhn, K Lambeck, MT Nhuan, D Qin and PL Woodworth. (2001) Changes in sea level. In: Houghton, J.T., Ding, Y., Griggs, D.J., Noguer, N., Van der Linden, P.J. & Xiaou, D. (eds.) *Climate change 2001: The scientific basis*. Cambridge University Press, Cambridge, UK.

DeSantis LRG, Bhotika S, Williams K, Putz FE (2007) Sea-level rise and drought interactions accelerate forest decline on the Gulf Coast of Florida, USA. Global Change Biology **13**: 2349-2360.

Domec J-C, A Noormets, JS King, G Sun G, SG McNulty et al. (2009) Decoupling the influence of leaf and root hydraulic conductances on stomatal conductance and its sensitivity to vapor pressure deficit as soil dries in a drained loblolly pine plantation. Plant, Cell Enviro **32**:980-991.

Domec J.C., J. S King, E. Ward, A. C. Oishi, S. Palmroth, A. Radecki, D. M. Bell, G. Miao, M. Gavazzi, D. M. Johnson, S.G. McNulty, G. Sun, A. Noormets (2015) Conversion of natural forests to managed forest plantations decreases tree resistance to prolonged droughts. Forest Ecology and Management **355**:58-71.

Domec, J.-C., Palmroth S., Oren. R (2016) Effects of *Pinus taeda* leaf anatomy on vascular and extravascular leaf hydraulic conductance as influenced by N-fertilization and elevated CO_2. Journal of Plant Hydraulics **3**e007.

Ehlert C, C Maurel, F Tardieu and C Simonneau (2009) Aquaporin-Mediated Reduction in Maize Root hydraulic conductivity impacts cell turgor and leaf elongation even without changing transpiration. Plant Physiology **150**: 1093-1104.

Else M.A., Coupland D., Dutton L. & Jackson M.B (2001) Decreased root hydraulic conductivity reduces leaf water potential, initiates stomatal closure and slows leaf expansion in flooded plants of castor oil (*Ricinus communis*) despite diminished delivery of ABA from the roots to shoots in xylem sap. Physiologia Plantarum **111**, 46– 54.

Farquhar, G.D., S. von Caemmerer and J.A. Berry (1980) A biochemical model of photosynthetic CO2 fixation in leaves of C3 species. Planta **149**, 78-90

Gambetta G.A., Fei J., Rost T.L., Knipfer T., Matthews M.A., Shackel K.A., Walker M.A., McElrone A.J. (2013) Water uptake along the length of grapevine fine roots: developmental anatomy, tissue-specific aquaporin expression, and pathways of water transport. Plant Physiology **163**, 1254–1265.

Gambetta GA, Knipfer T, Fricke W, McElrone AJ (2017) Aquaporins and root water uptake. In: F Chaumont, S Tyerman (eds) Plant Aquaporins, Signaling and Communication in Plants. Springer Verlag Berlin, Heidelberg, pp 133– 153

Hacke UG, JS Sperry, BE Ewers, DS Ellsworth, KVR Schäfer, and R Oren (2000) Influence of soil porosity on water use in *Pinus taeda.* Oecologia **124**:495-505.

Henzler T, Steudle E. 2004. Oxidative gating of water channels (aquaporins) in *Chara* by hydroxyl radicals. Plant Cell & Environemnt 27: 1184-1195.

Holbrook NM and MA Zwieniecki (2003) Plant biology: water gate. Nature 425:361

Johnson D.M., M. Sherrard, J.C. Domec, R.B. Jackson (2014) Role of aquaporin activity in regulating deep and shallow root hydraulic conductance during extreme drought. Tree Structure and Function **28**:1223-1331.

Johnson D.M., Wortemann R., McCulloh K.A., Jordan-Meille L.,Ward E., Warren J.M., Palmroth S., Domec J.-C. (2016) A test of the hydraulic vulnerability segmentation hypothesis in angiosperm and conifer tree species. Tree Physiology **36**: *983-993*.

Kamaluddin M and JJ Zwiazek (2002) Ethylene enhance water transport in hypoxic aspen. Plant Physiology **128**:962-969.

651 **Keeland, BD and R R Sharitz** (1995). Seasonal growth patterns of *Nyssa sylvatica* var. biflora,
652 *Nyssa aquatica*, and *Taxodium distichum* as affected by hydrologic regime. Canadian Journal of
653 Forest Research **25**:1084–1096.
654
655 **Kirwan ML, Gedan KF** (2019) Sea-level driven land conversion and the formation of ghost
656 forests. Nature Climate Change: **9**: 450-457.
657
658 **Knifer T and Fricke W** (2011) Water uptake by seminal and adventitious roots in relation to
659 whole-plant water flow in barley (*Hordeum vulgare* L.). Journal Experimental Botany **62**:717-
660 33.
661
662 **Kozlowski TT.** (1997) Responses of woody plants to flooding and salinity. Tree Physiology
663 Monograph **1**:1–29.
664
665 **Krauss KW, JL Chambers, JA Allen, B Luse and A DeBosier.** (1999) Root and shoot responses
666 of *Taxodium distichum* seedlings subjected to saline flooding. Environmental and Experimental
667 Botany **41**:15-23.
668
669 **Leyton** L and Z **Rousseau**. (1958) Root growth of tree seedlings in relation to aeration. In:
670 Thimann, K.V. (ed.), The physiology of forest trees. Ronald Press, New York. p. 467–475.
671
672 **Li X., X. Wang, Y. Yang, R. Li, Q. He, X. Fang, D. Luu, C. Maurel, J. Lin** (2011) Single-
673 Molecule Analysis of PIP2;1 Dynamics and Partitioning Reveals Multiple Modes of *Arabidopsis*
674 Plasma Membrane Aquaporin Regulation. The Plant Cell **23** :3780-3797
675
676 **Loustau D, S Crepeau, MG Guye, M Sartore, E Saur.** (1995) Growth and water relations of
677 three geographically separate origins of maritime pine (*Pinus pinaster*) under saline conditions.
678 Tree Physiology **15**: 569-576
679
680 **Martinez-Ballesta M.C., Martinez V., Carvajal M** (2000) Regulation of water channel activity
681 in whole roots and in protoplasts from roots of melon plants grown under saline conditions.
682 Australian Journal of Plant Physiology **27**, 685–691.
683
684 **Maurel C, Nacry P** (2020) Root architecture and hydraulics converge for acclimation to changing
685 water availability. Nature Plants **6**:744–749.
686
687 **McCulloh K., Domec J-C, Johnson D.M., Smith D.D., Meinzer F.C.** (2019) A dynamic yet
688 vulnerable pipeline: Integration and coordination of hydraulic traits across whole plants. Plant,
689 Cell & Environment **42***:* 2789-2807 DOI: 10.1111/pce.13607**.**
690
691 **McElrone A. J., Bichler, J., Pockman, W. T., Addington, R. N., Linder, C. R., & Jackson, R.**
692 **B.** (2007). Aquaporin-mediated changes in hydraulic conductivity of deep tree roots accessed via
693 caves. Plant, Cell & Environment **30**, 1411–1421.
694

McLean E.H., Ludwig, M., Grierson, P. F. 2011. Root hydraulic conductance and aquaporin abundance respond rapidly to partial root-zone drying events in a riparian *Melaleuca* species. *New Phytologist.* **192**, 664–675.

McLeod KW, JK McCarron, and WH Conner (1996) Effects of flooding and salinity on photosynthesis and water relations of four Southeastern Coastal Plain forest species. Wetlands Ecology and Management **4**: 31-42.

Megonigal JP and FP Day (1992) Effects of flooding on root and shoot production of bald cypress in large experimental enclosures. Ecology **73**: 1182-1193.

Meinzer FC (2003) Functional convergence in plant responses to the environment. Oecologia **134**:1-11.

Miao, G., Noormets, A., Domec, J.-C., Trettin, C.C., McNulty, S.G., Sun, G., King, J.S (2013) The effect of water table fluctuation on soil respiration in a lower coastal plain forested wetland in the southeastern US. J. Geophys. Res.: Biogeosci. **118**, 1748–1762.

Munns R (2002) Comparative physiology of salt and water stress. Plant Cell Envir **25**:239–50.

Munns R and M Tester (2008) Mechanisms of salinity tolerance. Annu. Rev. Plant Biol. 2008. **59**:651–81

NAS (2020) *Climate Change: Evidence and Causes: Update 2020*. Washington, DC: The National Academies Press. 36p. https://doi.org/10.17226/25733.

Niinemets U (2010) Responses of forest trees to single and multiple environmental stresses from seedlings to mature plants: Past stress history, stress interactions, tolerance and acclimation. Forest Ecology and Management **260**: 1623-1639.

Oppenheimer, M., B.C. Glavovic , J. Hinkel, R. van de Wal, A.K. Magnan, A. Abd-Elgawad, R. Cai, M. Cifuentes-Jara, R.M. DeConto, T. Ghosh, J. Hay, F. Isla, B. Marzeion, B. Meyssignac, and Z. Sebesvari. (2019) Sea Level Rise and Implications for Low-Lying Islands, Coasts and Communities. In: IPCC Special Report on the Ocean and Cryosphere in a Changing Climate [H.-O. Pörtner, D.C. Roberts, V. Masson-Delmotte, P. Zhai, M. Tignor, E. Poloczanska, K. Mintenbeck, A. Alegría, M. Nicolai, A. Okem, J. Petzold, B. Rama, N.M. Weyer (eds.)].

Oren R, Sperry JS, Katul GG, Pataki DE, Ewers BE, Phillips N and KVR. Schäfer (1999) Survey and synthesis of intra- and interspecific variation in stomatal sensitivity to vapour pressure deficit. Plant Cell Environment **22**:1515–1526.

Peltier WR (2002) On eustatic sea level history: last glacial maximum to Holocene. Quaternary Science Reviews **21**: 377-396.

Pezeshki SR (1992) Response of *Pinus taeda* to soil flooding and salinity. Annales des Sciences Forestières **4**: 149-159.

Poulter B, NL Christensen and Q.S. Song (2008) Tolerance of *Pinus taeda* and *Pinus serotina* to low salinity and flooding: Implications for equilibrium vegetation dynamics. Journal of Vegetation Science **19**: 15-22.

Rodríguez-Gamir, J., Ancillo, G., Legaz, F., Primo-Millo, E. & Forner-Giner, M.A (2012) Influence of salinity on PIP gene expression in citrus roots and its relationship with root hydraulic conductance, transpiration and chloride exclusion from leaves. *Environmental and experimental botany* **78**, 163–166

Rodriguez-Gamir J., Xue J., Clearwater M.J., Meason D.F., Clinton P.W. & Domec J.-C (2019) Aquaporin regulation in roots controls plant hydraulic conductance, stomatal conductance and leaf water potential in *Pinus radiata* under water stress. *Plant, Cell & Environment* **42**:717-729. DOI: 10.1111/pce.13460.

Ross MS and JJ O'Brien (1994) Sea-level rise and the reduction in pine forests in the Florida Keys. Ecological Applications **4**:144-156.

Siefritz F, MT Tyree, C Lovisolo, A Schubert and R Kaldenhoff (2002) PIP1 plasma membrane aquaporins in tobacco; from cellular effects to function in plants. The Plant cell **14**:869-876.

Sperry JS. (2003) Evolution of water transport and xylem structure. International Journal of Plant Science **164**: 115–127.

Tan X, Zwiazek JJ. (2019) Stable expression of aquaporins and hypoxia-responsive genes in adventitious roots are linked to maintaining hydraulic conductance in tobacco (Nicotiana tabacum) exposed to root hypoxia. *PLoS One*. **14**(2):e0212059.

Titus JG and C. Richman (2001) Maps of lands vulnerable to sea level rise: modeled elevations along the US Atlantic and Gulf coasts. Climate Research 18: 205-228.

Törnroth-Horsefield S, Y Wang, K Hedfalk, U Johanson, M Karlsson, E Tajkhorshid, R Neutze and P. Kjellbom (2006) Structural mechanism of plant aquaporin gating. Nature **439**:688-694

Tyree MT, Sinclair B, Lu P, Granier A. 1993. Whole shoot hydraulic conductance in Quercus species measured with a new high-pressure flow meter. Ann. For Sc. **50**: 417-423.

Tyree MT and MH. Zimmermann (2002) Xylem Structure and the Ascent of Sap (second ed), Springer, New York, NY.

Vandeleur, R. K., Sullivan, W., Athman, A., Jordans, C., Gilliham, M., Kaiser, B. N., & Tyerman, S. D (2014). Rapid shoot-to-root signalling regulates root hydraulic conductance via aquaporins. *Plant, Cell & Environment* **37**, 520–538. ttps://doi.org/10.1111/pce.12175

Ward, E.J., Oren, R., Bell, D.M., Clark, J.S., McCarthy, H.R., Seok-Kim, H., Domec, J.-C (2013) The effects of elevated CO2 and nitrogen fertilization on stomatal conductance estimated from scaled sapflux measurements at Duke FACE. Tree Physiol **33**, 135–151.

Yang, S. and M.T. Tyree (1994) Hydraulic architecture of *Acer saccharum* and *A. rubrum*: comparison of branches to whole trees and the contribution of leaves to hydraulic resistance. J. Exp. Bot. **45**:179-186.

Ye, Q., & Steudle, E (2006). Oxidative gating of water channels (aquaporins) in corn roots. Plant, Cell & Environment ***29***, 459–470. https://doi.org/10.1111/j.1365-3040.2005.01423.x

Zhang J., Zhang X (1994) Can early wilting of old leaves account for much of the ABA accumulation in flooded leaves? J. Exp. Bot. **45**: 1335-1342.

Figure captions

Figure 1: Mean values (+SE) of hydraulic conductances (solid bars) in root, shoot and whole loblolly pine (n=6) and bald cypress (n=5) plants growing in control, droughted, flooded and flooded + salt conditions. Crosses indicate a significant difference between control and any of the treatments (p<0.05). Hashed bars represent values of hydraulic conductance following aquaporin inhibition i.e. the xylem-only part of the hydraulic pathway.

Figure 2: Partitioning of hydraulic resistances (1/conductance) of loblolly pine and bald cypress organs in control, flooded and flooded + salt conditions. Note that in all cases root and leaves represented more than 70% of total whole plant resistance.

Figure 3: Effect (shown in percent) of either the xylem-only (structural changes in xylem conduits) or the aquaporin-only (AQP) part of the hydraulic pathway on the decrease in loblolly pine and bald cypress hydraulic conductance between control and drought, flooded, and flooded plus salinity treatments (absolute values of conductances are seen in Fig. 1). For a given stress applied, the structural part of the hydraulic pathway reducing conductance was calculated by dividing the difference in conductance between control and treatment after inhibiting AQP activity by the difference in conductance between control and treatment without inhibiting AQP activity. The AQP effect was taken as 1 minus the structural effect. Bars with patterns represent treatments that did not induce significant difference in conductance (p>0.05; flooded condition for bald cypress).

Figure 4: Aquaporin (AQP) contribution to root, stem, leaf and whole-plant hydraulic conductances in (A) loblolly pine (n=6, +SE) and (B) bald cypress seedlings (n=5, +SE) growing under control, water-stressed, flooded, and flooded plus salinity conditions. Crosses indicate a significant difference in whole-plant AQP contribution between control and any of the treatments (p<0.05).

Figure 5: (A) Linear relationship between the maximum (reference) stomatal conductance (g_s at vapor pressure deficit = 1 kPa) and (B) plant hydraulic conductance (K_{plant}) and between the sensitivity of stomatal conductance to vapor pressure deficit ($dg_s/dlnVPD$) and $g_{s\text{-}max}$ of plant species growing under control, water-stressed, flooded, and flooded plus salinity conditions.

832 Circles, diamonds, squares and triangles represent bald cypress, water tupelo, loblolly pine and red
833 maple, respectively. Crossed-filled symbols represent mature plants growing in the field, non-
834 crossed symbols represent bald cypress and loblolly pine seedlings from the greenhouse
835 experiment. In (B), the red line (slope = 0.6) indicates the theoretical slope between stomatal
836 conductance at VPD = 1 kPa and stomatal sensitivity to VPD that is consistent with the role of
837 stomata in regulating minimum leaf water potential (Oren et al. 1999).
838
839 Figure 6: Maximum stomatal conductance ($g_{s\text{-}max}$) and the sensitivity of stomatal conductance to
840 vapor pressure deficit ($dg_s/dlnVPD$) versus percent of hydraulic resistance in roots of bald cypress
841 (Bald.) and loblolly pine (L.-Pine) seedlings growing under control, water-stressed, flooded, and
842 flooded plus salinity conditions.
843
844 Figure 7: Maximum stomatal conductance ($g_{s\text{-}max}$) and Light saturated photosynthetic rate (A_{sat})
845 versus aquaporin (AQP) contribution to root, or whole-plant hydraulic conductances of bald
846 cypress (Bald.) and loblolly pine (L.-Pine) seedlings growing under control, water-stressed,
847 flooded, and flooded plus salinity conditions.

Table 1. Plant, root (fine and coarse), stem and leaf dry masses (g), as well as mean tracheid diameters (Dt_stem; Dt_root), fine-root to leaf mass ratio ($Root_{fine}$/Leaf), and leaf mass per area (LMA) for the different treatments of *Taxodium distichum* (n=5, +SE) *and Pinus taeda* (n=6, +SE). The presence (Yes - and the percentage of roots affected) or absence (No) of root aerenchyma (intercellular air spaces) observed 5 weeks after initiating the treatments is also indicated.

	Control		Drought		Flooded		Flooded plus Salt	
	T. distichum	*P. taeda*	*T. distichum*	*P. taeda*	*T. distichum*	*P. taeda*	*T. distichum*	*P. taeda*
Plant (g)	13.9 ± 1.1C	10.7 ± 0.4B	9.9 ± 0.9AB	9.1 ± 0.4A	11.7 ± 1.0BC	9.5 ± 0.6A	9.7 ± 0.8AB	7.9 ± 0.8A
Root (g)	6.1 ± 0.4B	4.7 ± 0.4A	4.4 ± 0.5A	4.2 ± 0.3A	5.0 ± 0.6AB	4.9 ± 0.4A	3.9 ± 0.5A	4.3 ± 0.3A
Stem (g)	5.4 ± 0.5D	2.9 ± 0.2B	3.3 ± 0.3C	2.2 ± 0.1A	3.9± 0.4 C	1.9 ± 0.2 A	2.8 ± 0.2B	1.8 ± 0.1A
Leaf (g)	2.4 ± 0.6AB	3.1 ± 0.4B	2.2 ± 0.4B	2.6 ± 0.3B	2.8 ± 0.8AB	2.7 ± 0.3B	2.9 ± 0.7AB	1.7 ± 0.3A
Dt_stem (µm)	23.1±3.8C	14.8±2.1B	19.9±2.2C	9.4±1.2A	22.6±4.1C	13.6±1.5AB	17.8±2.2BC	10.2±1.5A
Dt_root (µm)	12.3±0.9C	10.2±1.0BC	11.8±1.3C	8.8±0.8AB	13.3±1.6C	9.0±0.6B	10.7±1.1BC	7.6±0.5A
Aerenchyma	Yes – 38 %	No	No	No	Yes – 84 %	No	Yes – 24 %	No
$Root_{fine}$/Leaf	0.72 ± 0.09B	0.53 ± 0.05A	0.74 ± 0.10B	0.50 ± 0.06A	0.71 ± 0.12AB	0.67 ± 0.04B	0.48 ± 0.07A	0.79 ± 0.9B
LMA (g cm^{-2})	9.1 ± 0.9B	13.4 ± 0.7D	7.0 ± 0.6A	11.8 ± 0.5C	8.9 ± 1.0B	11.4 ± 0.8C	7.2 ± 0.4A	9.0 ± 0.6B

Values in horizontal sequences not followed by the same letter are significantly different at the 0.05 level.

Table 2: Mean root hydraulic conductance on a root-mass basis ($K_{root\_biomass}$), root hydraulic conductance on a root-mass basis after inhibiting aquaporin (AQP) activity (AQP-inhibited $K_{root\_biomass}$), leaf water potentials (Ψ_{leaf}), stomatal conductance, light saturated photosynthesis, and photosynthetic parameters at 25°C (VC_{max25}, J_{max25}, R_{d25}) for the different treatments of *Taxodium distichum and Pinus taeda*. Values are means +SE (n=5-6).

	Control		Drought		Flooded		Flooded plus Salt	
	T. distichum	*P. taeda*	*T. distichum*	*P. taeda*	*T. distichum*	*P. taeda*	*T. distichum*	*P. taeda*
$K_{root\_biomass}$ ($g\ kg^{-1}\ s^{-1}\ MPa^{-1}$)	8.6 ± 0.3C	9.6 ± 1.1C	5.9 ± 0.4B	4.6 ± 0.7A	8.0 ±1.2C	5.4 ± 0.7AB	5.0 ± 1.4AB	3.3 ± 1.2A
AQP-inhibited $K_{root\_biomass}$ ($g\ kg^{-1}\ s^{-1}\ MPa^{-1}$)	3.9 ± 0.3A	5.6 ± 0.7B	4.0 ± 0.1A	3.8 ± 0.7A	3.4 ±0.4A	5.1 ± 0.6B	3.7 ± 0.5A	3.1 ± 0.7A
Predawn water potential (MPa)	-0.32 ± 0.02B	-0.24 ± 0.01A	-0.78 ± 0.07C	-0.93 ± 0.08C	-0.31 ± 0.02B	-0.39 ± 0.05B	-0.71 ± 0.09C	-0.77 ± 0.09C
Midday water potential (MPa)	-0.70 ± 0.08A	-1.18 ± 0.07B	-0.94 ± 0.09A	-1.29 ± 0.07B	-0.78 ± 0.09A	-1.22 ± 0.11B	-0.98 ± 0.06A	-1.38 ± 0.10B
Stomatal conductance (g_{s_max}, $mmol\ m^{-2}\ s^{-1}$)	124 ± 13E	93 ± 6D	92 ± 11D	41 ± 5B	115 ± 7DE	61 ± 6C	49 ± 9BC	25 ± 3A
Light saturated photosynthetic rate ($A_{sat:}$ $\mu mol\ m^{-2}\ s^{-1}$)	7.0 ± 0.5C	6.1 ± 0.4C	4.2 ± 0.5B	4.3 ± 0.6B	6.2 ± 0.7C	4.4 ± 0.8B	3.3 ± 0.5B	1.8 ± 0.2A
Rubisco carboxylation capacity ($VC_{max25,}$ $\mu mol\ m^{-2}\ s^{-1}$)	44.9 ± 6.2D	33.2 ± 5.2CD	25.3 ± 3.4BC	21.7 ± 2.5B	34.9 ± 3.8CD	26.0 ± 1.6B	10.8 ± 2.4A	6.1 ± 0.9A
Maximum electron transport rate ($J_{max25,}$ $\mu mol\ m^{-2}\ s^{-1}$)	66.3 ± 5.6D	52.3 ± 4.1C	39.1 ± 3.2B	32.5 ± 3.3B	55.7 ± 6.1CD	38.6 ± 5.2B	29.6 ± 6.6B	13.3 ± 1.4A
Dark respiration rate ($R_{d25,}$ $\mu mol\ m^{-2}\ s^{-1}$)	0.22 ± 0.04BC	0.27 ± 0.04C	0.19 ± 0.04B	0.17 ± 0.02B	0.19 ± 0.02B	0.23 ± 0.04BC	0.12 ± 0.02A	0.10 ± 0.01A

Values in horizontal sequences not followed by the same letter are significantly different at the 0.05 level.

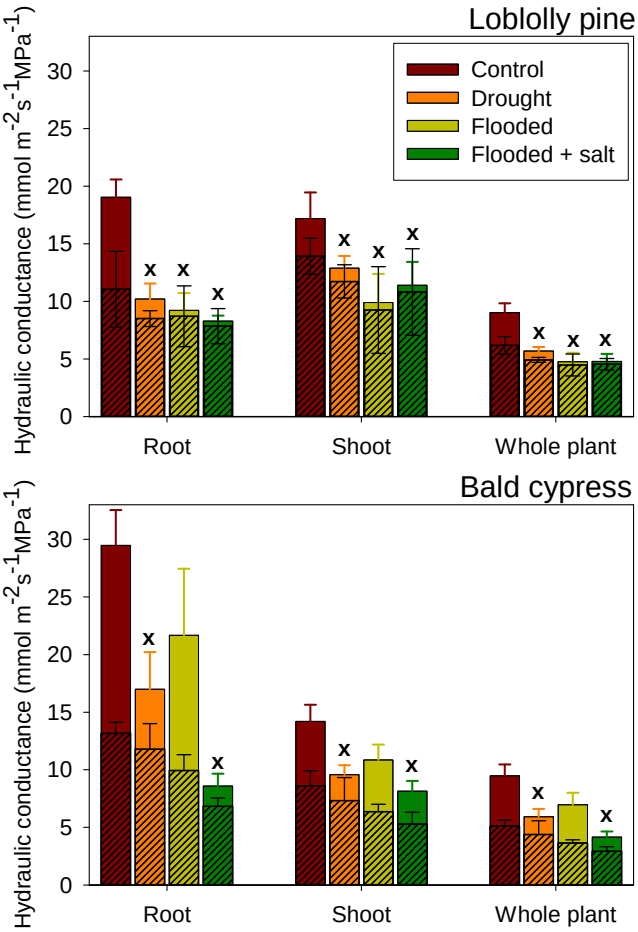

Figure 1: Mean values (+SE) of hydraulic conductances (solid bars) in root, shoot and whole loblolly pine (n=6) and bald cypress (n=5) plants growing in control, droughted, flooded and flooded + salt conditions. Crosses indicate a significant difference between control and any of the treatments (p<0.05). Hashed bars represent values of hydraulic conductance following aquaporin inhibition i.e. the xylem-only part of the hydraulic pathway.

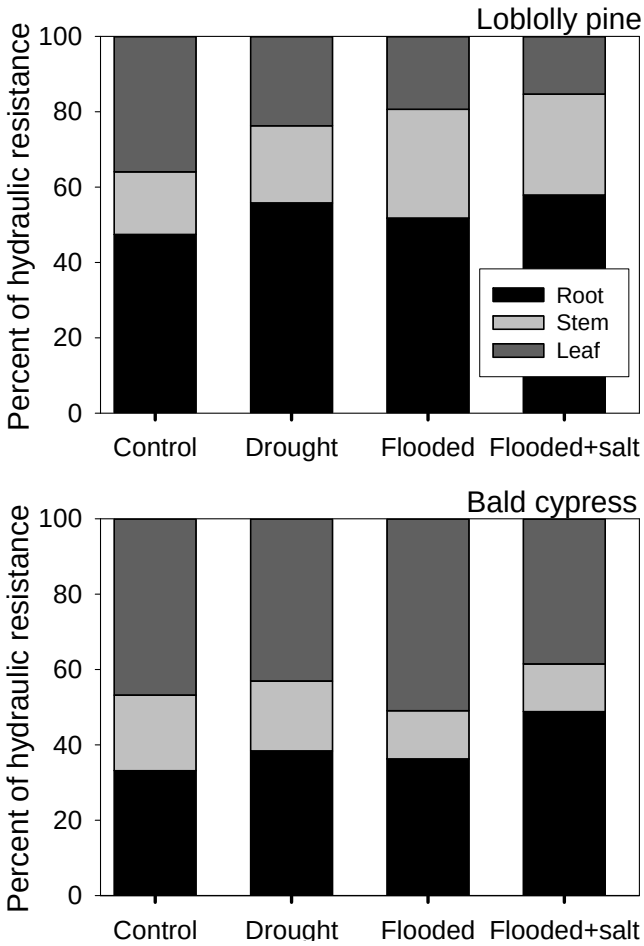

Figure 2: Partitioning of hydraulic resistances (1/conductance) of loblolly pine and bald cypress organs in control, flooded and flooded + salt conditions. Note that in all cases root and leaves represented more than 70% of total whole plant resistance.

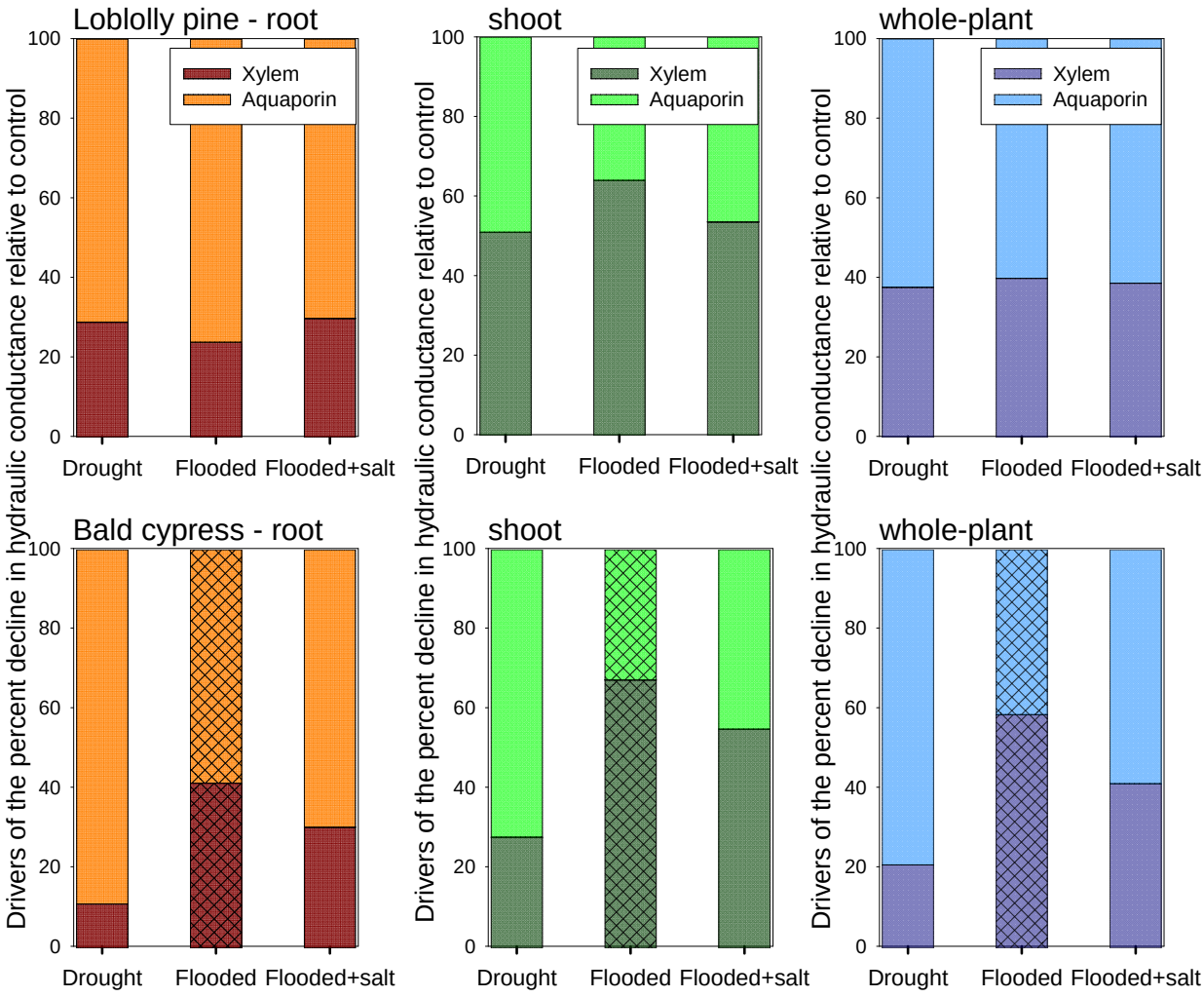

Figure 3: Effect (shown in percent) of either the xylem-only (structural changes in xylem conduits) or the aquaporin-only (AQP) part of the hydraulic pathway on the decrease in loblolly pine and bald cypress hydraulic conductance between control and drought, flooded, and flooded plus salinity treatments (absolute values of conductances are seen in Fig. 1). For a given stress applied, the structural part of the hydraulic pathway reducing conductance was calculated by dividing the difference in conductance between control and treatment after inhibiting AQP activity by the difference in conductance between control and treatment without inhibiting AQP activity. The AQP effect was taken as 1 minus the structural effect. Bars with patterns represent treatments that did not induce significant difference in conductance (p>0.05; flooded condition for bald cypress).

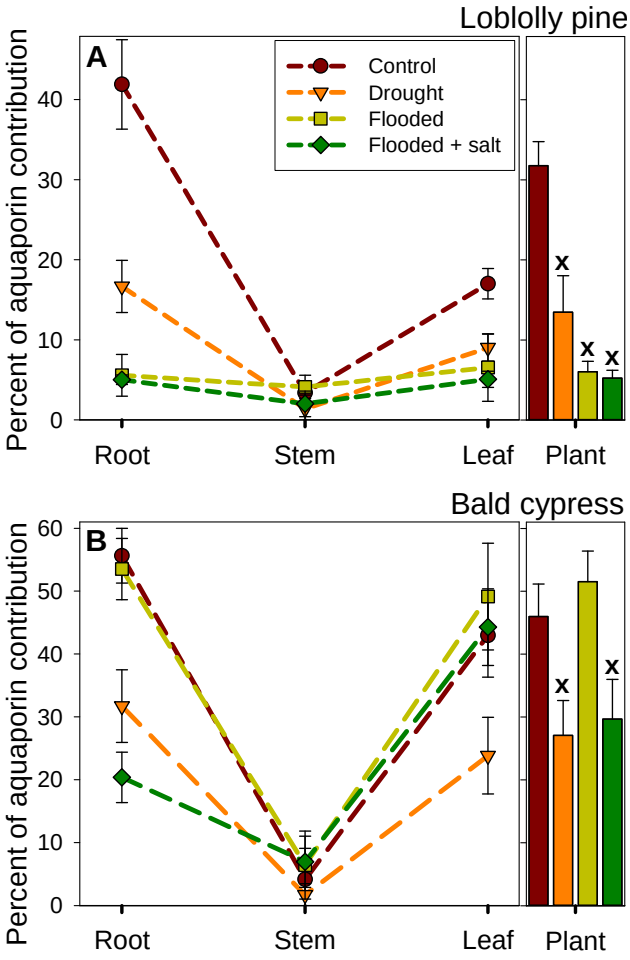

Figure 4: Aquaporin (AQP) contribution to root, stem, leaf and whole-plant hydraulic conductances in (A) loblolly pine (n=6, +SE) and (B) bald cypress seedlings (n=5, +SE) growing under control, water-stressed, flooded, and flooded plus salinity conditions. Crosses indicate a significant difference in whole-plant AQP contribution between control and any of the treatments (p<0.05).

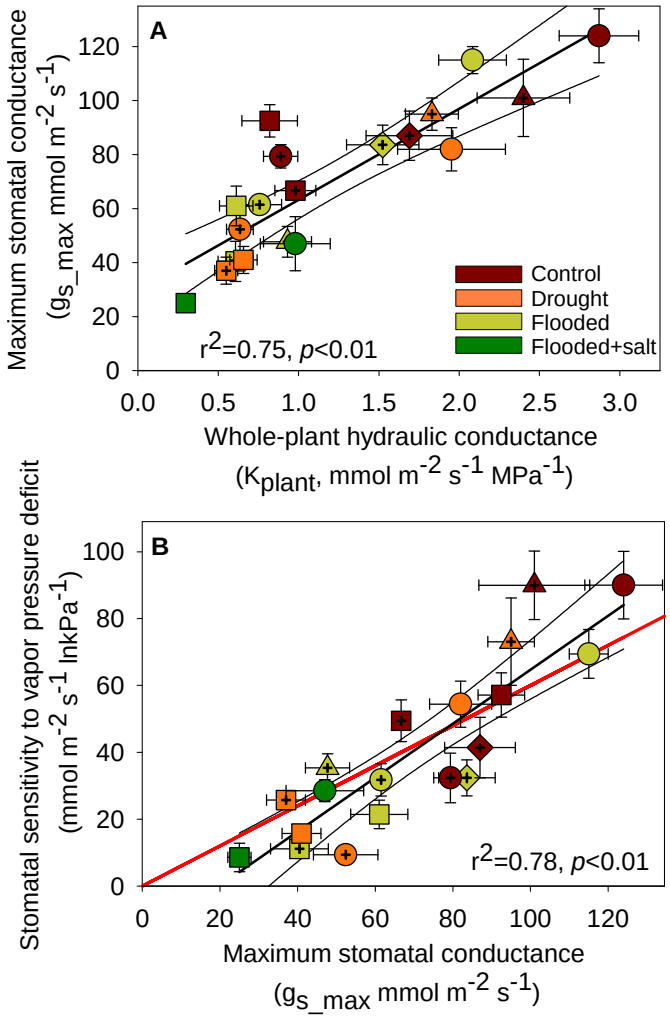

Figure 5: (A) Linear relationship between the maximum (reference) stomatal conductance (g_s at vapor pressure deficit = 1 kPa) and (B) plant hydraulic conductance (K_{plant}) and between the sensitivity of stomatal conductance to vapor pressure deficit ($dg_s/dlnVPD$) and $g_{s\text{-}max}$ of plant species growing under control, water-stressed, flooded, and flooded plus salinity conditions. Circles, diamonds, squares and triangles represent bald cypress, water tupelo, loblolly pine and red maple, respectively. Crossed-filled symbols represent mature plants growing in the field, non-crossed symbols represent bald cypress and loblolly pine seedlings from the greenhouse experiment. In (B), the red line (slope = 0.6) indicates the theoretical slope between stomatal conductance at VPD = 1 kPa and stomatal sensitivity to VPD that is consistent with the role of stomata in regulating minimum leaf water potential (Oren et al. 1999).

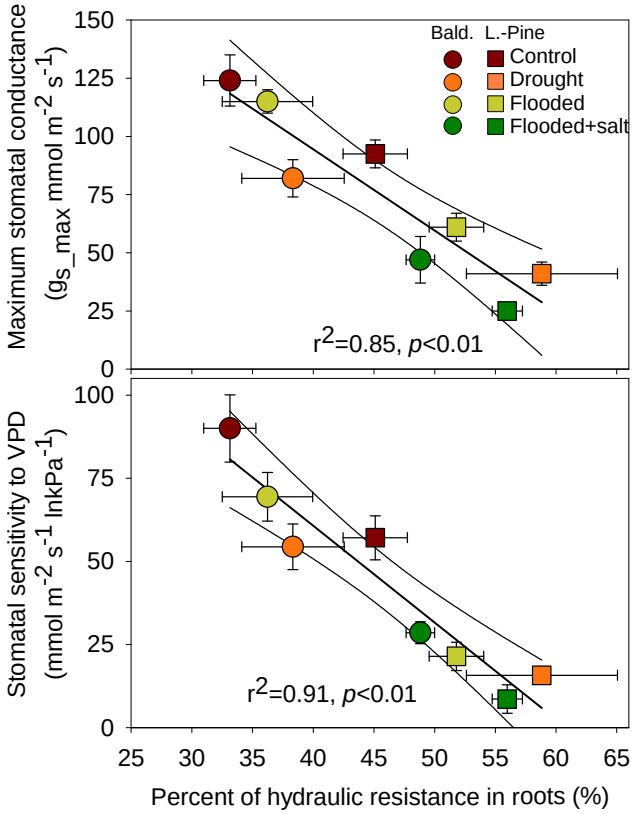

Figure 6: Maximum stomatal conductance ($g_{s\text{-}max}$) and the sensitivity of stomatal conductance to vapor pressure deficit (dg_s/dlnVPD) versus percent of hydraulic resistance in roots of bald cypress (Bald.) and loblolly pine (L.-Pine) seedlings growing under control, water-stressed, flooded, and flooded plus salinity conditions.

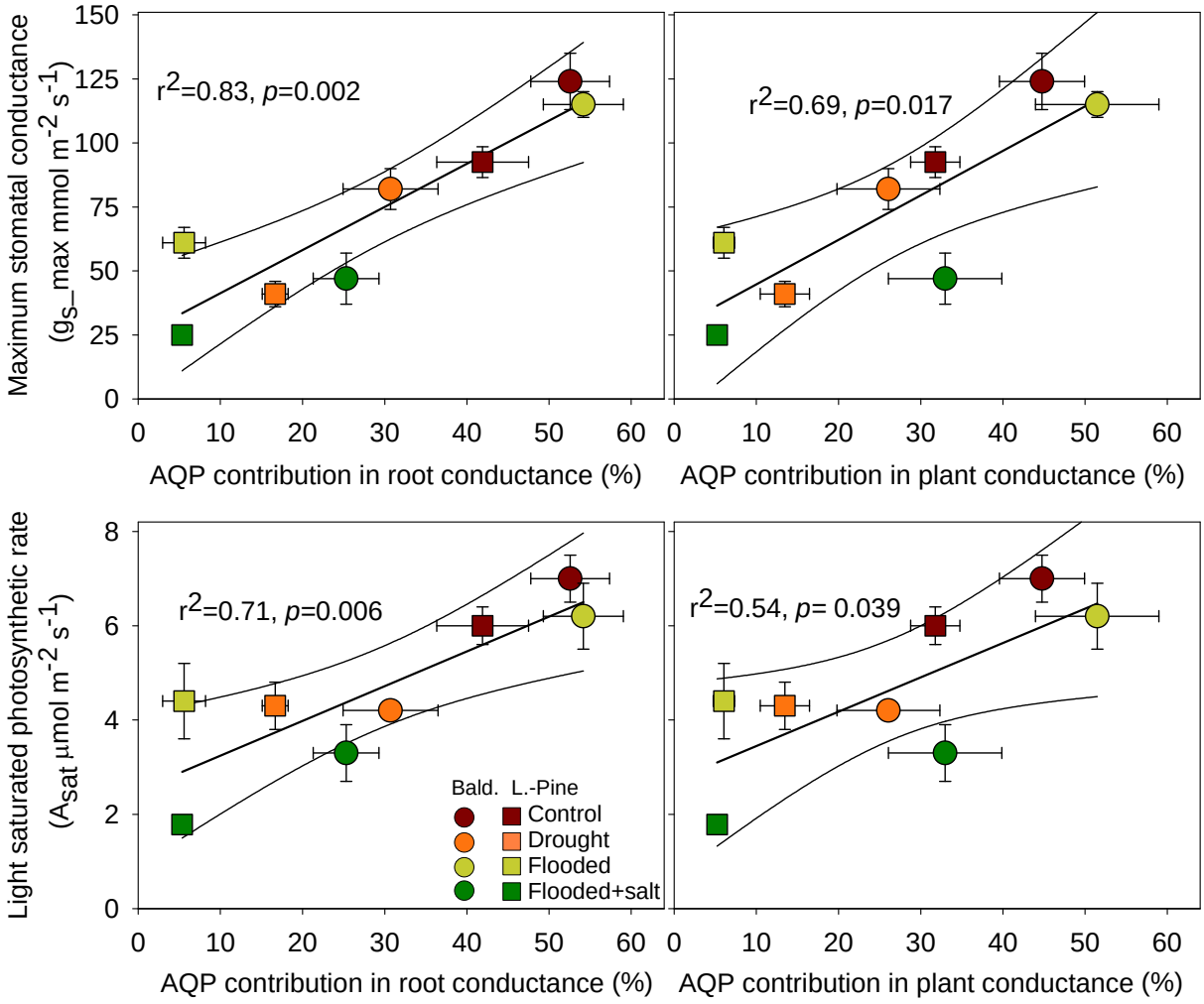

Figure 7: Maximum stomatal conductance ($g_{s\text{-}max}$) and light saturated photosynthetic rate (A_{sat}) versus aquaporin (AQP) contribution to root, or whole-plant hydraulic conductances of bald cypress (Bald.) and loblolly pine (L.-Pine) seedlings growing under control, water-stressed, flooded, and flooded plus salinity conditions.